Acoustic emission and lifetime prediction during static fatigue tests on ceramic-matrix-composite at high temperature under air

Sébastien Momon, Mariette Moevus, Nathalie Godin, Mohamed R'Mili, Pascal Reynaud, Gilbert Fantozzi, G. Fayolle

Acoustic emission and lifetime prediction during static fatigue tests on ceramic-matrix-composite at high temperature under air

S. Momon [a], M. Moevus [a], N. Godin [a,*], M. R'Mili [a], P. Reynaud [a], G. Fantozzi [a], G. Fayolle [b]

[a] Université de Lyon, INSA-Lyon, MATEIS, 7 Avenue Jean Capelle, 69621 Villeurbanne, France
[b] Snecma Propulsion Solide, Les Cinq Chemins, 33185 Le Haillan, France

The present work deals with two types of ceramic matrix composites CMC: SiC_f/[Si–B–C] and C_f/[Si–B–C], loaded in static fatigue at high temperature. An acoustic emission-based technique is proposed to predict the residual fatigue life. Indeed, two approaches based on the analysis of released energy are applied. A coefficient denoted R_{AE} is evaluated. Moreover, a cumulative Benioff law commonly used for pre-seismic activations is applied. Under constant stress, micro-cracks are created, which generate elastic waves in a manner similar to earthquakes. The law predicted satisfactorily the time-to-failure of SiC_f/[Si–B–C] composite under a constant load.

1. Introduction

Ceramic matrix composites (CMCs) are interesting structural materials for high temperature applications, since they retain good mechanical properties at elevated temperatures. Non-oxide ceramic matrix composites (CMCs), and more particularly SiC/SiC or C/SiC composites have been widely studied during the last decades [1–3]. Such fibre reinforced ceramic composites are very attractive candidates for many high-temperature structural applications, thanks to their high temperature strength and light weight. Future engine applications in civil aircrafts are foreseen for such composites [4], but these applications require very long lifetime in-service conditions. A big issue is therefore a better understanding of the damage mechanisms and kinetics in order to perform reliable life predictions. An assessment of the remaining lifetime of the structures is the goal of this work.

Concepts of statistical physics associated with phase changes and critical points have been successfully applied to a variety of problems. These models exhibit an avalanche behavior very similar to the one observed in seismicity. In 1962, early pioneering experiments on rocks are due to Mogi [5]. Acoustic emissions associated with micro-cracks were monitored and power law frequency–magnitude statistics were observed. This relation, known as the Gutenberg–Richter distribution, has been known for many years to describe the frequency–magnitude statistics of earthquakes [6]. Geologists have found that the number of earthquakes of magnitude M is proportional to 10^{-bM}. They call this law the Gutenberg–Richter law. Thus, Mogi (1962) found similarities between AE activity and earthquake occurrence. He demonstrated that in many ways the statistical behavior of micro-fracturing activity observed in laboratory experiments is similar to that observed for earthquakes. Hirata [7] showed that the acoustic emission prior to failure of a rock followed a power law spatial distribution. Similar results were obtained by Lockner [8]. Many researchers investigated the elastic energy release during the failure process of materials. Smith and Phoenix [9], Curtin [10] and Newman and Phoenix [11] studied the critical point hypothesis (CPH) by using fibre model. Turcotte and Shcherbakov [12] and Ben-Zion and Lyakhovsky [13] also performed analogous investigation on CPH. They got the analytical expression of energy release process under constant loading. The results indicated that prior to material failure, energy release would accelerate in the form of a power law. Johansen and Sornette [14] studied the rupture of spherical tanks made with Kevlar wrapped around thin metallic liners. They found that the increase of acoustic emission prior to rupture follows a power law. Guarino et al. [15] studied the failure of circular panels of chipboards and fibre glass. He showed that the frequency–magnitude statistics of acoustic emission also satisfy the power law (Gutenberg–Richter). Prior to failure of materials, distinct critical phenomena will appear, the latter being considered as precursors for the failure of rock materials and the occurrence of large earthquakes. This damage acceleration before failure is detected by AE monitoring during the fracturing of heterogeneous material (Guarino et al. [16], Sornette and Andersen [17], Nechad et al. [18]). Deschanel et al. [19,20] showed on polyurethane foam that fitting time intervals with a power law seems to require a quasi constant constraint during most of the test. In tension, a competition

* Corresponding author. Tel.: +33 472 438 073; fax: +33 472 438 528.
E-mail address: nathalie.godin@insa-lyon.fr (N. Godin).

between relaxation times that are specific to material, and characteristic time imposed by the deformation rate is observed. On the other hand, in static fatigue when a constant loading is applied, the specimen elongates freely. The released AE energy is always power law distributed independently of material porosity, loading history or mechanical properties.

Usually, when a sample is loaded below its strength, there is a time delay before failure. This delay is due to the occurrence and coalescence of micro-cracks which generate acoustic emission of broad amplitude. Acoustic signals should thus provide an indirect measure of damage. Acoustic emission (AE) is also useful to obtain additional information on damage mechanisms and on their kinetics during static fatigue. The acoustic emission (AE) technique seems to be a very appropriate tool to detect in situ information about damage occurring during mechanical tests. An important question in materials science is to identify the precursors of ultimate failure. Therefore, a main tool is the detection by AE monitoring of micro-fractures occurring before failure.

In this study, C_f/[Si–B–C] and SiC_f/[Si–B–C] composites with self-healing matrix were studied under static fatigue under air at temperatures of 700 °C, 1000 °C and 1200 °C for the C_f/[Si–B–C] composite and at 450 °C and 500 °C for the SiC_f/[Si–B–C] composite. In order to protect the interface against oxidation, matrix contains phases which produce sealants at high temperatures preventing oxygen from reaching the interphase. AE was recorded during the tests. A main purpose of this study was to consider the possibility of predicting rupture time from damage evolution recorded by AE technique. It has been observed that an increase in the seismic activity, prior to large earthquakes, is described by a power law. This was first proposed by Bufe and Varnes [21,22]. The cumulative Benioff "strain" (the sum of the square root of the energy released for sequential earthquakes) has been suggested as a precursory phenomenon of large earthquakes, increasing as an inverse power law of time before the main shock. This precursory phenomenon is similar to the evolution of damage in a material during the tertiary creep stage. In this paper, results derived previously from the problem of seismic activation prior to earthquakes are applied on CMC. The first two sections focus on a review of the experimental and data-processing procedures. Typical experimental results are given in the third section. Two approaches based on the analysis of liberated energy are applied. A coefficient denoted R_{AE} is defined in order to describe the evolution of AE activity during test. Applicability of the Benioff's law to lifetime prediction is examined from a qualitative point of view.

2. Materials

Both composite materials have a multilayered [Si–B–C] matrix reinforced and an PyC interface layer. They are reinforced with different fibres: Hi-Nicalon fibres for the first one and carbon fibres (ex PAN-HR) for the second one. These composites were manufactured by SNECMA Propulsion Solide (Bordeaux, France). The multilayered matrix was made by chemical vapour infiltration from the ternary [Si–B–C] system. The external surface was protected by a seal coat. The fibres perform consisted of stacked woven clothes (fibre volume fraction of 35–40% and a porosity volume fraction of about 12%). The test specimens were dog-bone shaped with following dimensions: 4 mm in thickness, 16 mm in width, gauge length of 30 mm for the C_f/[Si–B–C] and 40 mm for SiC_f/[Si–B–C], and a cross section of 64 mm^2.

3. Experimental procedure

3.1. Mechanical testing

Static fatigue tests on the C_f/[Si–B–C] composite were conducted under uni-axial tensile loading, and the axis of loading was parallel to one direction of fibres. These tests were performed at 700 °C, 1000 °C and 1200 °C under air using a servo-hydraulic testing system (INSTRON 8502) with an inductive furnace. Before loading, the specimen was heated up to the testing temperature at a rate of 50 °C/min and held during 30 min to achieve uniform temperature distribution at the gauge section prior to the beginning of the test. For each test, the first loading was applied with a constant loading rate of 1kN/min, and during the tests, unloading/reloading sequences were done periodically (every 6 h or 12 h according to the duration of the test). For the SiC_f/[Si–B–C] composite, static fatigue experiments were performed on a pneumatic testing machine at 450 °C or 500 °C under air. The specimens were loaded at a constant rate of 600 N/min up to a constant stress chosen in the range of 45–100% of σ_R, σ_R being the stress to failure. Specimen elongation was measured using a high temperature extensometer and AE was recorded.

3.2. AE data acquisition system

AE was monitored by using a MISTRAS 2001 data acquisition system (Euro Physical Acoustics). For the tests at 450 °C or 500 °C under air on the pneumatic machine, two MICRO-80 sensors were positioned directly on the specimen, 190 mm apart, inside the grips. Medium viscosity vacuum grease was used as a coupling agent. The acquisition parameters were set as follows: preamplification 40 dB, threshold 32 dB, peak definition time 50 μs, hit definition time 100 μs, hit lockout time 1000 μs.

For the tests above 700 °C performed on the hydraulic machine, two wave guides made of heat-resistant steel with a length of 140 mm and a diameter of 8 mm were put on the specimen 100 mm distant. Each wave guide was attached to the corresponding MICRO-80 sensor, using vacuum grease as a coupling agent. The acquisition parameters for the two active channels were set as follows: preamplification 40 dB, threshold 48 dB, peak definition time 50 μs, hit definition time 100 μs and hit lockout time 1000 μs. In both cases, AE signal parameters (amplitude, energy, duration, counts, average frequency, rise time and location) as well as time, load and strain were measured in real time by the data acquisition system.

For AE origin identification, AE wave velocity was determined before the test, using a pencil break procedure: several were broken on the specimen at various locations between the sensors. The difference in time of arrival at the sensors was calculated using the first peak of each signal. The AE wave velocity was found to be equal to 3200 m/s for the C_f/[Si–B–C]. For the SiC_f/[Si–B–C] composite, the initial velocity was found to be equal to 10,000 m/s. The difference in these two speeds results from the differences between the two composites investigated (different fibres) and from the use of wave guides on the hydraulic testing machine.

4. AE analysis: data processing

From all the signals detected in the gauge length, it is possible to follow and characterize the global energy of acoustic emission during the tests. It is interesting to quantify this energy in order to assess the amount of damage of the composites. The energy of the recorded AE events represents a part of the elastic energy released by CMC specimens. Thus, we can investigate the evolution of elastic energy released by analyzing the energy of AE events. We propose to define the coefficient of emission R_{AE} as the increment of energy ΔE recorded during an increment of time Δt (Fig. 1), divided by the total energy emitted during the initial loading of the sample:

$$R_{AE}(t) = \frac{1}{E_{loading}} \frac{\Delta E}{\Delta t} \quad (1)$$

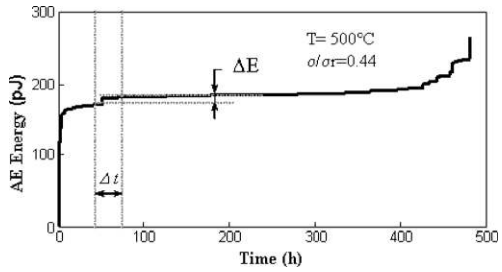

Fig. 1. AE activity in terms of cumulative AE energy released during a static fatigue test for the composite SiC_f/[Si–B–C] at 500 °C.

where $E_{loading}$ is the cumulative AE energy for all the signals recorded during the initial loading up to the nominal load of the test, ΔE is the cumulative AE energy for all signals recorded during the interval $[t; t + \Delta t]$.

Benioff's law [21,22] (the sum of the square root of the energy released for sequential earthquakes) has been suggested for precursory phenomena of large earthquakes, increasing as an inverse power law of time before a main shock.

$$\Omega(t) = \sum_{i=1}^{N(t)} \sqrt{E_i} = \Omega_c + B(t_c - t)^{1-\gamma} \quad (2)$$

where E_i is the seismic energy release of the ith precursory earthquake and $N(t)$ is the number of precursory earthquakes considered up to time t. Ω_c is the value of $\Omega(t) = \sum_{i=1}^{N(t)} \sqrt{E_i}$ when $t = t_c$, t_c is the critical time. $B = -\frac{\varphi}{1-\gamma}$ is negative, $1 - \gamma$ is an exponent and ϕ is a constant. The time-to-failure model is a technique in which a failure function is fitted to a time series of cumulative Benioff strain before a large earthquake.

Based on Eq. (2), the increase of AE collected during fatigue is analyzed. E_i is the energy of the ith AE signal detected and $N(t)$ is the number of AE signals recorded and located along the gauge length until time t, t_c is the failure time. In this study, the proposed log-periodic corrections of the power law [23] were not done.

5. Results and discussion

5.1. Evolution of the coefficient of emission R_{AE}

Fig. 1 exhibits a typical evolution of the AE energy released during a static fatigue test when a dramatic increase before failure is observed. The AE activity (defined here as the cumulative AE energy) plotted in Fig. 1, was recorded for a specimen of SiC_f/[Si–B–C] loaded at $\sigma\sigma_R = 0.44$. The main activity occurred at the beginning of the test. Then the AE rate decreased to a minimum and steeply increased before failure. This typical evolution is often observed, but not systematically. Nevertheless, this resumption of AE seems to be an interesting way of anticipating the final failure. The acoustic activity seems to give precursory signs of rupture by a renewal of activity. This phenomenon is better observed by representing the acoustic energy released versus time steps. This increment of energy is the coefficient of emission R_{AE} which was defined in Section 4. The time step was chosen so that the less noisy curve was obtained. The optimal value is about 10% of the duration of test.

The evolution of R_{AE} coefficient versus time is given on Figs. 2 and 3 in logarithmic coordinates, for the two CMCs of this study. In both cases, the R_{AE} coefficient decreases first, down to a minimum value for $t = t_m$, and then it increases up to the failure of the composite at time t_c. This ultimate increase in the AE activity was not always obvious on the global curves of AE energy versus time (unlike in Fig. 1), but was systematically revealed by the

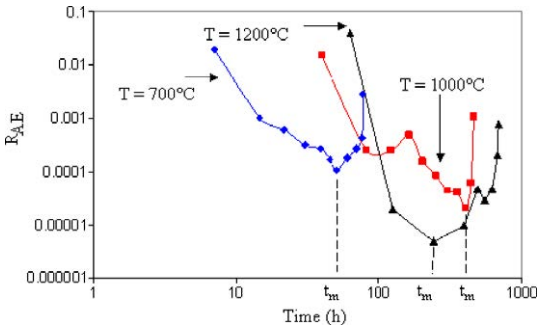

Fig. 2. Evolution of the R_{AE} coefficient during the static load hold for the composite C_f/[Si–B–C] at high temperatures 700 °C, 1000 °C and 1200 °C.

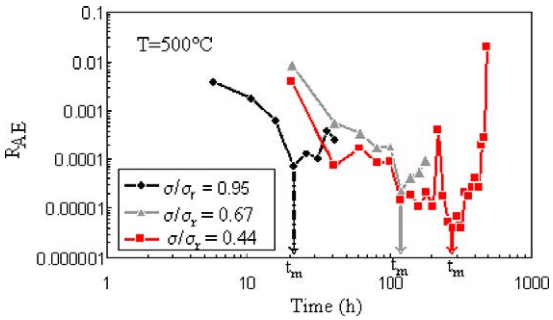

Fig. 3. Evolution of the R_{AE} coefficient during the static load hold for the composite SiC_f/[Si–B–C] at 500 °C loaded at several σ/σ_r ratios.

R_{AE}. Thus, according to the critical point hypothesis [11], the energy release, prior to failure of CMC materials, would accelerate. The ratio t_m/t_c is given in Table 1 for several $\sigma\sigma_R$ ratios for the composite SiC_f/[Si–B–C]. It is noticed that t_m/t_c is less scattered: the mean value is about 0.59 and the standard deviation is 0.05, which is low. Thus, the R_{AE} indicator is a promising way to detect the renewal of acoustic activity and to anticipate the rupture of composite.

The ratio t_m/t_c was determined for several temperatures for the composite C_f/[Si–B–C] (see Table 2). In this case, the existence of a minimum for the R_{AE} coefficient of emission was observed for all the tests. These results confirm that the R_{AE} indicator allows detection of the renewal of acoustic activity and anticipation of the rupture. But for this composite, under static fatigue at 700 °C or 1000 °C, this minimum was detected at approximately 71% ± 8% of the specimen lifetime. A higher scattering of time appears at 1200 °C, the R_{AE} indicator varies between 40% and 85% due to a lower acoustic activity at this temperature. For the C_f/[Si–B–C] composites, the minimum of R_{AE} is relatively reproducible for a given temperature but occurs on average later than for the SiC_f/[Si–B–C] composites. Thus, the instant corresponding to the minimum of R_{AE} seems to be linked to temperature and material type.

Table 1
Values of ratio t_m/t_c for several $\sigma\sigma_R$ ratios SiC_f/[Si–B–C].

T (°C)	σ/σ_r	t_m (h)	t_c (h)	t_m/t_c
500	0.95	26	42.5	0.61
500	0.91	71	136	0.52
500	0.79	121	195	0.62
500	0.71	61	109	0.56
500	0.67	21	42	0.50
500	0.44	300	480	0.63
450	0.95	242	372	0.65
450	0.91	366	591	0.62
Mean value				0.59
Standard deviation				0.05

Table 2
Values of ratio t_m/t_c for several $\sigma\sigma_R$ ratios in the case of C_f/[Si–B–C].

T (°C)	σ/σ_r	t_m (h)	t_c (h)	t_m/t_c
700	0.52	220	345	0.64
700	0.60	50	78	0.65
700	0.68	5.5	8	0.68
1000	0.60	335	465	0.72
1000	0.68	70	91	0.77
1000	0.86	4.5	6	0.79
1200	0.57	275	687	0.40
1200	0.65	122	144	0.85
Mean value				0.69
Standard deviation				0.14

For CMC, the renewal of activity at the end of the tests may be attributed to the avalanche fibres ruptures, controlled by the oxidation of fibres and by the recession of interfaces, slowed down by the self-healing matrices.

So, the monitoring of acoustic emission enables to anticipate the rupture of the sample, thanks to the detection of more and more energy signals at the end of the test. When a minimum of activity in energy (not an inflection) is highlighted, this minimum being obtained for a time $t_m = kt_c$ with $k < 1$, a minimum value of the R_{AE} indicator, can be detected leading to an assessment of the lifetime t_c.

On the SiC_f/[Si–B–C] composite, the AE data were analyzed using an unsupervised multi-variable clustering method [24,25], which is able to reveal the natural structures of the data. In previous papers [24,25], AE signals have been correlated with the damage mechanisms which occur in these CMCs. These results are summarized in the present paper. It has been pointed out that several types of signals can be distinguished, and that the obtained clusters are consistent with the expected differentiation of damage mechanisms. According to the Davies and Bouldin criterion, an optimal clustering was obtained with four clusters noted A–D ranked by energy. The A-type signals are the biggest ones, i.e. highest energy, duration and amplitude. The B-type signals can be distinguished for their lower energy, higher rise time to duration ratio and higher apparent frequency when compared to the cluster A. The clusters C and D exhibit quite the same low energy but C presents the shortest rise time, whereas D has the longest ones. The corresponding waveforms are thus really different. The signals of type A appeared mainly at the beginning of the tests, during initial loading. So, they were attributed to matrix cracking; these cracks propagated through several matrix layers and were the biggest cracks observed. Some A-type signals were also recorded just before ultimate failure of CMC in the failure zone of specimen. This suggests that cluster A contains also signals associated with the ultimate fracture, such as yarn fractures or collective fibre breaks (individual fibre breaks will be instead associated to the cluster B of lower energy). The B-type signals were also detected at the beginning of initial loading, and they were associated with another type of matrix cracking (cracks inside the transverse yarns). This type of signal was also detected during the load hold step until ultimate fracture in the area of fracture zone. These last B-type signals were mainly attributed to fibre breaks. The C-type signals are characterized by a low energy (short rise time and low amplitude). They were mainly detected during initial loading and were attributed to matrix cracks in the longitudinal yarns which are the shortest cracks. The D-type signals seem to be a consequence of the existing damage, and were logically related to fibre–matrix interfacial debonding.

In order to determine the class corresponding to the most significant failure precursors, R_{AE} was calculated for each class (see Fig. 4). The R_{AE} coefficients obtained for the two classes A and B go through a minimum, contrary to those of classes C and D. For

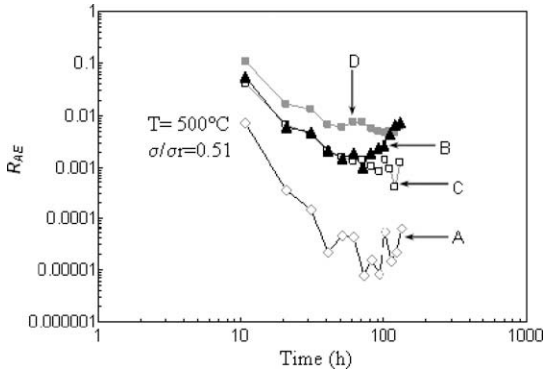

Fig. 4. Evolution of the R_{AE} coefficient during the static load hold for the composite SiC_f/[Si–B–C] for each damage mechanisms. (A: matrix cracks crossing several matrix layers with yarn's fracture or collective fibre breaks, B: matrix cracks in transverse yarn and individual fibre failure, C: matrix cracks in axial yarn and D: fibre–matrix interfacial debonding.)

the B class (mainly fibre failure at the end of the tests), the average ratio t_m/t_c is equal to 0.65 with a standard deviation of 0.10 (to be compared with a mean value of 0.59 and a standard deviation of 0.05 in Table 1). For the A class (mainly yarn fractures or collective fibre breaks at the end of the tests), the average ratio t_m/t_c is also equal to 0.65 with a standard deviation of 0.10. To obtain results which are comparable to those of the global analysis, it is necessary to take into account the two classes A and B, which contain the most energetic signals highly active at the end of the static fatigue tests. This result points out that it is not necessary to identify the numerous mechanisms in order to determine the minimum of R_{AE}. It is sufficient to consider the collective aspect of AE.

5.2. Application of the Benioff's law to assess the lifetime of the CMCs

In order to evaluate the lifetime of the composites, the Benioff's law was applied to the AE data recorded during the static fatigue tests at high temperatures. This law is based on a description by a power law of the cumulative energy (Ω) released by the composite (see Eq. (2) Section 4) characterized by four parameters (Ω_c, γ, φ and t_c). The AE data can be plotted in the log $(\Omega_c - \Omega) = f$ (log $(t_c - t)$) diagram, Ω_c being the square root of the total energy released at the end of the test (t_c). This allows us to cheek whether the energy released follows a power law and to estimate γ and φ by fitting the experimental results by the Benioff's law. It can be noticed first that the data beyond the minimum of R_{AE} show a better agreement with the Benioff's law (Fig. 5b) than those before the minimum of R_{AE} (Fig. 5a). That is why only the data collected beyond the minimum of R_{AE} were used in this study to assess life time. The Benioff's law parameters were then estimated using linear regression technique in log–log plot (Fig. 5). Fig. 6 gives the experimental curve and the one obtained from the Benioff's law and it shows an example of fit obtained using Eq. (2) for C_f/[Si–B–C] AE data set. On the basis of this good fit, it can be logically expected that appropriate predictions could be obtained by extrapolation of acoustic emission data using the empirical power law relation that an observable variable such as energy is supposed to follow. One can draw up an estimate of the time-to-failure (t_c) of the composite by using the following procedure: (1) Determination of Benioff's law parameters (Ω_c, γ, φ and t_c) from the AE data recorded until the rupture, using the representation log $(\Omega_c - \Omega) = f(\log(t_c - t))$. (2) Estimation of t_c using a partial AE data set, this set corresponding to data recorded between a time t_m and the time t, with t lower than t_c and equal to $t_m + n\Delta t$, where Δt is arbitrarily chosen. The coefficient R_{AE} reaches a minimum value for $t = t_m$. Then the linear fit is applied to the truncated file in order

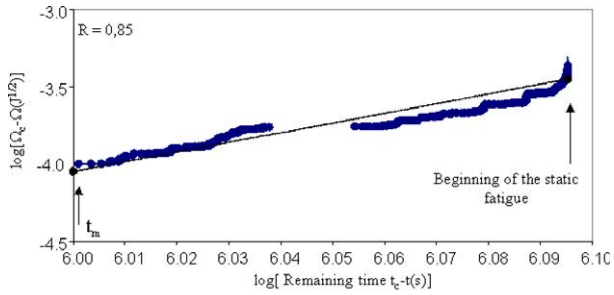

(a) Before the minimum of R_{AE}

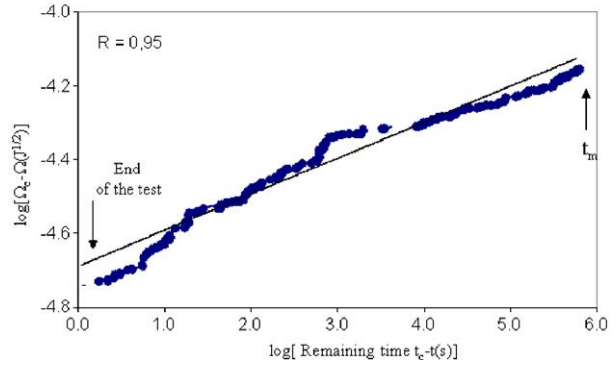

(b) After the minimum of R_{AE}

Fig. 5. The power law relation between AE energy versus the remaining time until failure. The regressive line represents the power law relation: (a) before the minimum of R_{AE} and (b) after the minimum of R_{AE}. (C_f/[Si–B–C] at 700 °C and $\sigma/\sigma_r = 0.52$).

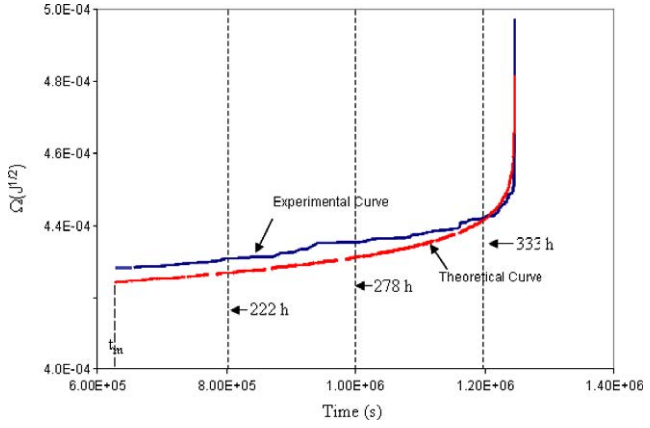

Fig. 6. Energy released in terms of Benioff Strain and its fitting with the Benioff law. (C_f/[Si–B–C] at 700 °C and $\sigma/\sigma_r = 0.52$).

to deduce t_c as one of the four variables of this fit (Ω_c, γ, φ and t_c) by the least-squares method modelling the portion of the experimental curve between t_m and t. This procedure then allows the time to rupture to be determined. In Table 3, the assessed values obtained at various times t are compared with the experimental values. For example, for the static fatigue test performed (700 °C to 130 MPa) on the C_f/[Si–B–C] composite, the law makes it possible to obtain an evaluation of t_c which is 17% under estimated from the data above 64% of lifetime. Obviously, the estimate of the lifetime becomes more and more accurate as t is close to the end of the test and reaches an accuracy of about 1% a few hours before rupture. Moreover, the AE data collected on SiC_f/[Si–B–C], using the same procedure, lead to an estimate of the time-to-failure with a much

Table 3
Comparison between the experimental values of t_c(exp) and the theoretical values t_c(th) obtained with Benioff's law.

	t (h)	t/t_c (exp.)	t_c (h) (theoretical)	t_c (th)/t_c (exp.)	$1-\gamma$
C_f/[Si–B–C]	222	0.64	289	0.83	0.1
T = 700 °C-	278	0.80	308	0.89	
σ/σ_r = 0.52	333	0.96	344	0.99	
SiC_f/[Si–B–C]	222	0.63	335	0.95	0.9
T = 500 °C	242	0.68	339	0.96	
σ/σ_r = 0.44	269	0.76	346	0.98	
	297	0.84	352	1.00	
	325	0.91	353	1.00	

better accuracy. This is due to the test temperature and the damage mechanisms that enhance emission. Indeed, for the static fatigue test performed on the SiC_f/[Si–B–C] composite, the law makes it possible to obtain an evaluation of t_c which is 5% under estimated, from the data above 63% of lifetime. We can note that the exponents $(1-\gamma)$ were very different for both composites ($1-\gamma = 0.1$ for C_f/[Si–B–C] and $1-\gamma = 0.9$ for SiC_f/[Si–B–C]). This suggests that even if the law is considered universal, the parameters are material dependent and they can be sensitive to the experimental conditions. Sornette [26] found that the value of the exponent associated with a critical phase transition is equal to 0.5. The exponent $(1-\gamma)$ is approximately equal to 0.25 for Rundle [27], 1/3 for the damage rheology model [13].

Thus, Benioff's law, which was initially used to study the activation of seisms or earthquakes, can also be applied to the damage of composites. However, this procedure requires to calibrate the law for a given CMC, with a test performed until rupture in order to obtain the four parameters. If the coefficients values are completely unknown, especially Ω_c, which corresponds to the total energy released at the end of the test, the evaluation of t_c will require longer calculations. For the evaluation of t_c from Benioff's law, t_c depends on three parameters (Ω_c, γ, φ) and is very sensitive to the values of Ω_c and the exponent $(1-\gamma)$. For a given material, the value of the exponent $(1-\gamma)$ is less scattered than Ω_c. The model based on Benioff's law provides a satisfactory approximation of the acceleration of the process of the AE release after the minimum of the R_{AE} coefficient. This result suggests that as the damage increases, especially after the minimum of R_{AE} coefficient, a new stage appears leading to ultimate fracture. For the SiC_f/[Si–B–C] composite and the C_f/[Si–B–C] composite, this avalanche phenomenon is certainly linked to the delayed failure of fibres [28] (slow crack growth, oxidation). The results indicate that an accuracy of a few percents on the evaluation of rupture time is obtained using AE recorded 40% before the rupture time of a composite. Nevertheless, this evaluation is done for given testing conditions and sample geometry. Sizes effects are not taken into account and should be investigated [29].

6. Conclusion

The elastic energy released during static fatigue tests was found to accelerate before ultimate failure regardless of experimental conditions. The AE activity appears to be an interesting tool to anticipate final failure of the specimen. A criterion was defined, which allows prediction of the end of a static fatigue test from the AE activity during the first half of the test. So, the R_{AE} coefficient can be used as a criterion to assess the remaining lifetime of a CMC specimen under static loading. It appears to be a promising tool to perform shorter static fatigue experiments which could be interrupt once the minimum value of R_{AE} has been reached, rather than waiting for ultimate failure. In this way, the test duration could be divided by 1.5–2. Preliminary studies were also made on failure

prediction from increasing energy release. The Benioff's law was applied to static fatigue data for CMC specimens at high temperatures. The Benioff's law and experimental AE data enabled a reliable prediction of remaining life. Further work on the data recorded before the minimum of the R_{AE} coefficient would be interesting to determine if they follow the Benioff's law and if they can be correlated to lifetime.

Acknowledgments

The authors gratefully acknowledge Snecma Propulsion Solide, CNRS and DGA for supporting this work in the frame of the CPR: 'Modélisation, extrapolation, validation de la durée de vie des CMC'.

References

[1] Dalmaz A, Reynaud P, Rouby D, Fantozzi F, Abbe G. Mechanical behaviour and damage evolution during fatigue at high temperature of a 2,5D C_f/SiC composite. Compos Sci Technol 1998;58:693–9.
[2] Boitier G, Vicens J, Chermant JL. Tensile creep results on a C_f/SiC composite. Scripta Mater 1998;37:1–18.
[3] Holmes JW, Sorensen BF. Fatigue behaviour of continuous fiber reinforced ceramic matrix composites. in: Nair SV, Jakus K, editors. Elevated temperature mechanical behavior of ceramic matrix composites. Buttherworth Heineman; 1994.
[4] Lee SS, Nicholas LP, Zawada T. Fatigue damage mechanisms and environmental effects on the long-term performance of matrix composites. Mech Test Ceram Ceramic Compos, ASME 1997:117–55.
[5] Mogi K. Study of the elastic shocks caused by the fracture of heterogeneous materials and its relations to earthquake phenomena. Bull Earthq Res Inst 1962;40:125–73.
[6] Bowman David D, Sammis Charles. Intermittent criticality and the Gutenberg–Richter distribution. Pure Appl Geophys 2004;161:1945–56.
[7] Hirata T, Satoh T, Ito K. Fractal structure of spatial distribution of microfracturing in rock. Geophys J Roy Astr Soc 1987;90:369–74.
[8] Lockner D. The role of acoustic emission in the study of rock fracture. Int J Rock Mech Min Sci Geomech Abstr 1993;30:883–99.
[9] Smith RL, Phoenix SL. Asymptotic distributions for the failure of fibrous materials under series-parallel structure and equal load-sharing. J Appl Mech 1981;48:75–82.
[10] Curtin WA. Theory of mechanical properties of ceramic-matrix composites. J Am Ceram Soc 1991;74:2837–45.
[11] Newman SL, Phoenix WI. Time dependent fiber-bundles with local load sharing. Phys Rev E 2001;63(2). No. 021 507.
[12] Turcotte D, Shcherbakov R. Can damage mechanics explain temporal scaling laws in brittle fracture and seismicity? Pure Appl Geophys 2006;163:1031–45.
[13] Ben-Zion Y, Lyakhovsky V. Accelerated seismic release and related aspects of seismicity patterns on earthquakes faults. Pure Appl Geophys 2002;159:2385–412.
[14] Johansen A, Sornette D. Critical ruptures. Euro Phys J B 2000;18:163–81.
[15] Guarino A, Ciliberto S, Garcimartin A. Failure time and microcrack nucleation. Euro Phys Lett 1999;47:456–61.
[16] Guarino A, Garcimartin A, Ciliberto S. An experimental test of the critical behaviour of fracture precursors. Eur Phys J B 1998;6:13–24.
[17] Sornette D, Andersen JV. Scaling with respect to disorder in time-to-failure. Eur Phys J B 1998;1:353–7.
[18] Nechad H, Helmstetter A, El Guerjouma R, Sornette D. Andrade and critical time-to-failure laws in fiber-matrix composites: experiments and model. J Mech Phys Solids 2005;53(5):1099–127.
[19] Deschanel S, Vanel L, Vigier G, Godin N, Ciliberto S. Statistical properties of microcracking in polyurethane foams under tensile test. Int J Fract 2006;140(1–4):87–98.
[20] Deschanel S, Vanel L, Vigier G, Godin N, Ciliberto S. Experimental study of crackling noise: conditions on power law scaling correlated to fracture precursors. J Stat Mech: Theory Exp 2009. No. PO1O18.
[21] Bufe CG, Varnes DJ. Predictive modelling of the seismic cycle of the greater San Francisco Bay region. J Geophys Res 1993;98:9871–83.
[22] Kawada Y, Nagahama H. Cumulative Benioff strain-release, modified Omori's law and transient behaviour of rocks. Tectonophysics. 2006;424:157–66.
[23] Anifrani JC, Le Floch C, Sornette D, Souillard D. Universal log-periodic correction to renormalization group scaling for rupture stress prediction from acoustic emissions. J Phys I 1995;5(6):631–8.
[24] Moevus M, Rouby D, Godin N, R'Mili M, Reynaud P, Fantozzi G, et al. Analyse of damage mechanisms and associated acoustic emission in two SiC/[Si–B–C] composites exhibiting different tensile curves. Part I: Damage patterns and acoustic emission activity. Compos Sci Technol 2008;68(6):1250–7.
[25] Moevus M, Godin N, R'Mili M, Rouby D, Reynaud P, Fantozzi G, et al. Analyse of damage mechanisms and associated acoustic emission in two SiC/[Si–B–C] composites exhibiting different tensile curves. Part II: Unsupervised acoustic emission data clustering. Compos Sci Technol 2008;68(6):1258–65.
[26] Sornette D. Mean-field solution of a block-spring model of earthquake. J Phys I 1992;2(11):2089–96.
[27] Rundle JB, Klein W, Turcotte DL, Maladud BD. Precursory seismic activation and critical-point phenomena. Pure Appl Geophys 2000;157:2165–82.
[28] Gauthier W, Lamon J. Delayed failure of Hi-Nicalon and Hi-Nicalon S multifilament tows and single filaments at intermediate temperatures (500°C–800°C). J Am Ceram Soc 2009;92(3):702–9.
[29] Phoenix SL, Ibnabdeljalil M, Hui C-Y. Size effects in the distribution for strength of brittle matrix fibrous composites. Int J Solids Struct 1997;34:545–68.